AIP | Applied Physics Letters

Temperature-induced ductile-to-brittle transition of bulk metallic glasses

G. Li, M. Q. Jiang, F. Jiang, L. He, and J. Sun

Citation: Appl. Phys. Lett. **102**, 171901 (2013); doi: 10.1063/1.4803170
View online: http://dx.doi.org/10.1063/1.4803170
View Table of Contents: http://apl.aip.org/resource/1/APPLAB/v102/i17
Published by the American Institute of Physics.

Temperature-induced ductile-to-brittle transition of bulk metallic glasses

G. Li,[1] M. Q. Jiang,[2] F. Jiang,[1,a)] L. He,[1] and J. Sun[1]
[1]*State Key Laboratory for Mechanical Behavior of Materials, Xi'an Jiaotong University, Xi'an 710049, China*
[2]*State Kay Laboratory of Nonlinear Mechanics, Institute of Mechanics, Chinese Academy of Sciences, Beijing 100190, China*

(Received 17 March 2013; accepted 11 April 2013; published online 29 April 2013)

Uniaxial tensile and uniaxial compressive tests for Zr-based bulk metallic glasses (BMGs) were conducted at room and cryogenic temperatures, respectively. It was observed that both the change of macroscopic fracture mode from ductile shear fracture to brittle normal tensile fracture and microscopic fracture feature from micron-scaled vein patterns to nano-scaled dimples with decreasing test temperatures were identified, indicating a significant ductile-to-brittle transition (DBT) behavior. The mechanism of DBT behavior was revealed by the competition between the intrinsic critical shear strength τ_0 and critical tensile strength σ_0 at different temperatures. © *2013 AIP Publishing LLC*. [http://dx.doi.org/10.1063/1.4803170]

Bulk metallic glasses (BMGs) are expected not to undergo ductile-to-brittle transition (DBT) which was exhibited by most body-centered cubic (bcc) metal alloys at cryogenic temperatures because they lack dislocation structure and therefore have no dislocation-based deformation. Preliminary studies demonstrated that BMGs at cryogenic temperature exhibit an enhanced plasticity with a higher shear-band density in compression test,[1–5] but do not present clearly the plasticity as well ambient temperature in tension test with several shear bands even only one,[6,7] and flow plasticity deteriorated compared with room temperature in three-point bending tests.[8] Raghavan *et al.*[9] studied Charpy impact toughness of a Zr-based BMG at various temperatures, and the results showed that toughness at cryogenic temperatures is not severely degraded for as-cast samples but dramatically decreases for annealed samples, and DBT temperature is sensitive to the free-volume content. Therefore, the mechanical behaviors of BMGs at cryogenic temperatures need to be further studied in detail.

For crystalline alloys, plastic deformation is primarily shear-stress driven dislocation activity, and brittle fracture is usually associated with normal-stress caused cleavage as the dislocation emission and motion are restricted, whether a brittle or ductile behavior is operative depends on which process requires a smaller activation stress.[10–12] Unlike crystalline alloys, the plastic deformation of metallic glasses is achieved predominantly to the formation of shear band driven by shear stress, and the shear band is intimately related to initial free volume.[13–15] However, when BMGs with few free volume even almost no free volume such as sample annealed below glass-transition temperature, the dominant fracture mode is not shear but tensile failure.[8,9] Similarly, the BMGs at cryogenic temperatures will have smaller free volume due to decrease of the mean atomic distances[1,2,16,17] and the fracture mechanisms may be changed as well.[8] In this letter, a significant DBT behavior of BMGs was identified and the DBT behavior related with the competition between intrinsic critical shear strength T_0 and critical tensile strength σ_0 at different temperature was systematically discussed.

The $Zr_{52.5}Cu_{17.9}Ni_{14.6}Al_{10}Ti_5$ (Vit105) was fabricated by arc-melting high-purity Zr, Cu, Ni, Al in a Ti-gettered argon atmosphere, followed by drop casting into water-cooled copper mold. Tensile samples of dog-bone geometry with gauge dimensions of $1 \times 1.2 \times 6\,mm^3$ and compression samples with dimensions of $3.5 \times 3.5 \times 7\,mm^3$ were produced from 1.5 mm and 4 mm thick plates, respectively. In order to obtain similar free volume state and to remove residual stress, these tensile and compressive samples were sealed in evacuated quartz capsules and annealed 15 min at 593 K which was below the glass transition temperature T_g of 683 K. The combined results of x-ray diffraction (XRD), high resolution transmission electron microscopy (HRTEM), and differential scanning calorimetry (DSC) demonstrated that the annealing treatment below T_g had not introduced crystallization and only the free volume concentration was a little lower than that of as cast samples.[8] The uniaxial tension and uniaxial compression were conducted on a computer-controlled SUNS CMT 5105 (China) testing machine with a nominal strain rate of $1 \times 10^{-4}\,s^{-1}$ at 293 K, 173 K, and 77 K, respectively. After tests, the fracture surface of these tested samples was carefully investigated with scanning electron microscopy (SEM, JEOL Ltd JSM-6700F and HITACHI S-2700).

The tensile engineering stress-strain curves of these samples were given in Figure 1(a). All these samples displayed an initial elastic deformation behavior and failed at different fracture stress σ_T^F without obvious plastic deformation. At 293 K, the sample presented a high σ_T^F (~1704 MPa) along a single shear band plane with shear fracture angle θ_T of 56° as shown in Figure 2(a), which is typical shear fracture mode of BMGs.[18] At 173 K and 77 K, however, the sample had lower σ_T^F of 1388 MPa and 573 MPa, respectively, and both failed in a normal tensile fracture mode with tensile fracture plane approximately perpendicular to the stress axis (i.e., $\theta_T = 90°$) as shown in Figures 2(b) and 2(c). The compressive engineering stress-strain curves of these samples were presented in Figure 1(b). All these samples did not display obvious plastic deformation behavior and their fracture stress σ_C^F increased with decreasing temperature (Table I). At 293 K and 173 K,

a)Author to whom correspondence should be addressed. Electronic mail: jiangfeng@mail.xjtu.edu.cn

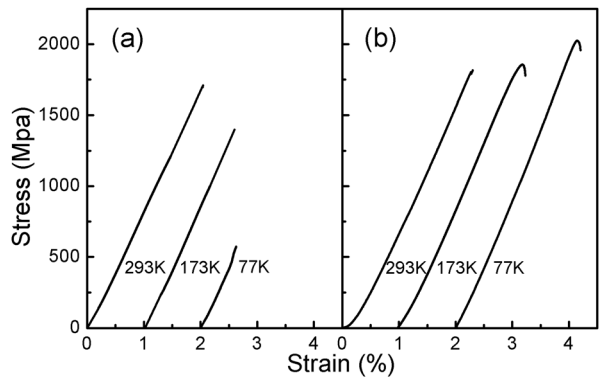

FIG. 1. Typical engineering stress-strain curves under (a) uniaxial tension and (b) uniaxial compression at temperatures ranging from 293 to 77 K.

samples failed in a shear mode with shear fracture angles θ_C of 43° as shown in Figures 2(d) and 2(e). With further decreasing temperature, however, the samples break into three pieces as shown in Figure 2(f). This fragmentation mode, i.e., split mode could also be found in other brittle BMGs (Mg, Fe, and Co based)[19–21] and annealed Zr-based BMGs[22] under compression.

Figure 3(a) illustrated that the fracture surface of the tensile sample failed in shear fracture mode at 293 K consisted of a dominant micron-scaled (~10 μm) cores and vein patterns. These micro-scaled cores and vein patterns were typical shear deformation and fracture feature of ductile metallic glasses under tension.[18,23] However, the fracture surface of the sample failed in normal tensile fracture mode at 173 K and 77 K displayed different features with the nano-scaled dimples rather than micron-scaled vein patterns as shown in Fig. 3(b) and 3(c). These nano-scaled dimples were typical fracture features of quasi cleavage brittle fracture of metallic glasses under tensile stress.[9,24–26] For the compressive samples which failed with shear fracture at 293 K and 173 K, micron scaled vein pattern regions were dominant in the two fracture surfaces, which are in agreement with these of other ductile BMGs.[18,23] While the samples failed in three pieces at 77 K, shear fracture surface with micron-scaled

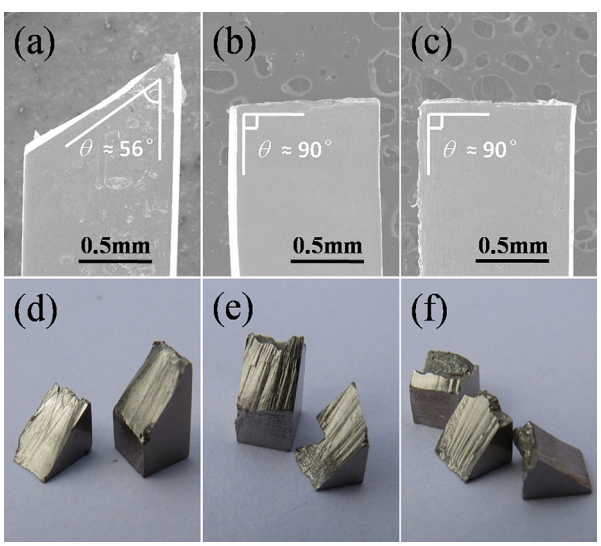

FIG. 2. Macroscopic fracture patterns of samples under ((a)-(c)) tension and ((d)-(f)) compression. (a) and (d) 293 K, (b) and (e) 173 K, (c) and (f) 77 K.

TABLE I. Mechanical properties and physical parameters of the BMG.

Temperature (K)	σ_C^F (MPa)	θ_C (°)	σ_T^F (MPa)	θ_T (°)	τ_0 (MPa)	σ_0 (MPa)	α
293	1817	43	1704	56	909	2606	0.33
173	1851	43	1388	90	926	1388	0.67
77	2030	43 and 90	573	90	1015	573	1.77

vein patterns and another fracture surface matched with nano-scaled vein dimples the same as tensile fracture surface shown in Figs. 3(b) and 3(c). Because the tensile stress gradually increased from zero due to volume dilation during the compression,[27] the sample should first shear to deformation, and then continue to fail in shear mode or tensile fracture in brittle mode, which are well agreement with the macroscopic fracture patterns and microscopic fracture feature.

Here, the ridge spacing (w) found on the fracture surface was used to estimate the fracture toughness (K_c) with the Dugdale approximation[26,28]

$$w = K_c^2/(6\pi\sigma_y^2), \tag{1}$$

where σ_y is yield strength and can be equal to σ_T^F for the present tensile tests. For the sample failed in shear fracture mode with scale of fracture surface pattern ~10 μm, the estimated K_c is about 23.4 MPa$\sqrt{\text{m}}$; For the sample failed in normal tensile fracture mode with fine dimples (~1.2 μm) even nano-scaled dimples (~80 nm), K_c are about 2.1 MPa$\sqrt{\text{m}}$ and 0.7 MPa$\sqrt{\text{m}}$, respectively.

Therefore, a significant DBT behavior had taken place according to the variation of fracture toughness as well as macroscopic fracture mode and microscopic fracture feature at different temperatures. It can be found that, as Figures 2 and 3, decreasing test temperature might change the macroscopic fracture mode from ductile shear fracture to brittle normal tensile fracture and microscopic fracture feature from micron-scaled vein patterns to nano-scaled dimples.

It is well recognized that fracture behaviors of materials are determined by the inherent competition between plastic flow by shear and volume dilation by crack propagation. Either plastic flow or crack propagation will occur, depending on which process requires the smaller applied stress, i.e., the shear stress and normal stress. Next, the intrinsic critical shear strength τ_0 and critical tensile strength σ_0 were calculated based on the tensile and compressive data as well as fracture angles in Table I, where τ_0 and σ_0 are defined as the critical strength of a material in a mode II fracture and the critical strength in a mode I failure, respectively.[29] Under compression, the shear fracture plane nearly made an angle close to 43° with respect to the compressive direction, even the split mode was first to shear along about 43° then to normal tensile fracture, it could be considered that the compressive fracture approximately followed the Tresca criterion. The compressive fracture strength could be simply expressed as $\sigma_C^F = 2\tau_0$. Following the unified fracture criterion,[29] $\sigma_T^F = 2\tau_0\sqrt{1-\alpha^2}$ $(\alpha = \tau_0/\sigma_0 \le \sqrt{2}/2)$ and $\sigma_T^F = \sigma_0 = \tau_0/\alpha$ $(\alpha = \tau_0/\sigma_0 \ge \sqrt{2}/2)$, then there was

$$\sigma_C^F/\sigma_T^T = 1/\sqrt{1-\alpha^2}\,(\alpha = \tau_0/\sigma_0 \le \sqrt{2}/2), \tag{2a}$$

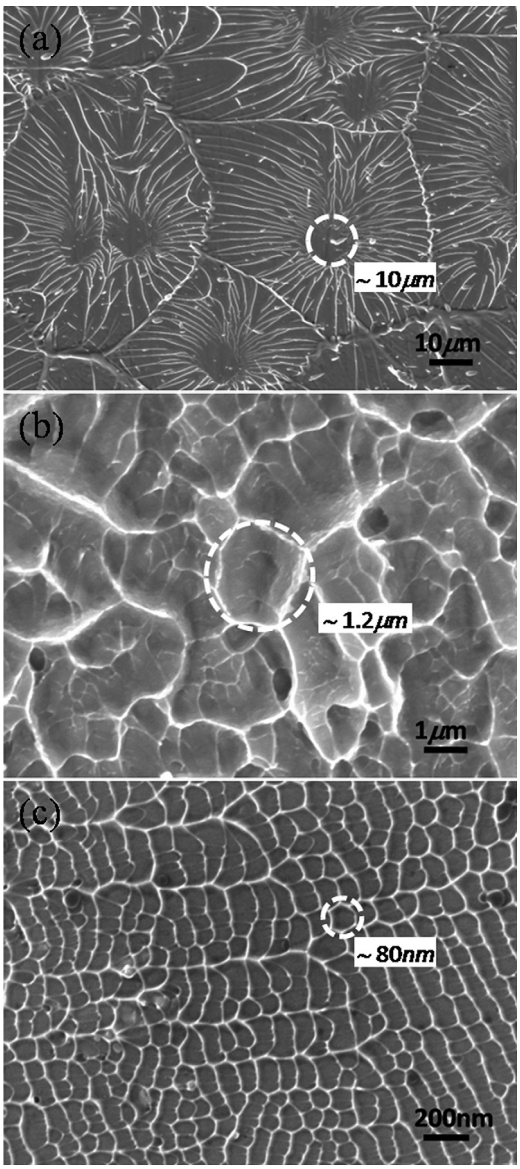

FIG. 3. SEM micrographs from the fracture surfaces of samples under tension. (a) 293 K, (b) 173 K, (c) 77 K. Length scales of vein patterns decrease with testing temperatures decreasing.

$$\sigma_C^F/\sigma_T^F = 2\alpha \ (\alpha = \tau_0/\sigma_0 \geq \sqrt{2}/2). \tag{2b}$$

After these, the τ_0, σ_0, and α were obtained through the measured values of σ_T^F, σ_C^F, θ_T, and θ_C, and were listed in Table I. It is to be noted here that samples tested at 173 K failed in brittle tensile fracture mode although the calculated $\alpha(0.67)$ is slight smaller than $\sqrt{2}/2$, this discrepancy might be due to the method for estimation of τ_0, where, Tresca criterion rather than Mohr-Coulomb criterion was used for simplicity.

Present results clearly showed that the critical shear strength τ_0 will slightly increase from ~909 MPa to about 1015 MPa (~10%) and the critical tensile strength σ_0 dramatically decrease from ~2606 MPa to ~573 MPa (~70%) with decreasing temperature as shown in Figure 4 and Table I. It means that the shear fracture (mode II failure) becomes more difficult and tensile fracture (mode I failure) is very apt to occur with decreasing test temperature, and at some critical value, the macroscopic mode of failure might change from

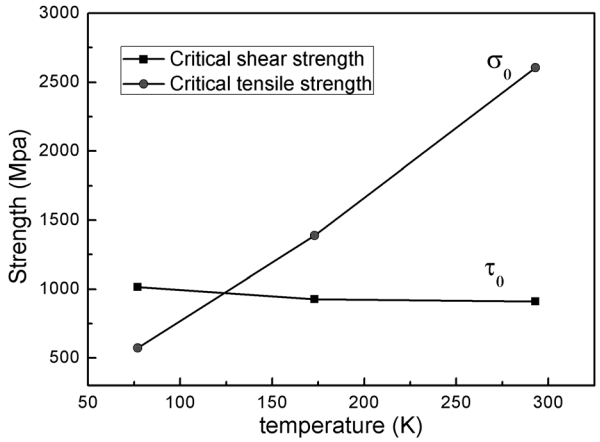

FIG. 4. Critical shear strength and critical tensile strength vs. temperatures.

ductile shear fracture to brittle tensile fracture. It is obvious that decreasing temperature will enhance the critical shear strength τ_0 and reduce the critical normal strength σ_0 to induce the DBT of BMGs.

The DBT behavior of crystalline alloys (e.g., body centered cubic metals and alloys) is due to the competition between the dislocation emission (flow) and cleavage (crack propagation). DBT of BMGs might be attributed to the competition between shear transformation zones (STZs) and tension transformation zones (TTZs).[24] The STZ operation actually is a local motion of atoms (clusters) around a free volume site as the unit process of plastic flow. While the TTZ is essentially a local atomic cluster similar in size to a STZ but with smaller relaxations timescales and less viscoplasticity, and the TTZ operation corresponds to the volume dilation through rupturing of cluster to form nano-scale void.[24] Thus, relation values of τ_0 and σ_0 will determine which process to be activated first between STZ and TTZ. If SZT is activated first, macroscopic flow of metallic glasses will occur as a result of a series of STZ operations to form shear band. In the opposite case, TTZ will form and large number of nano-scale void nucleation and coalescence produce new crack surfaces, then macroscopic brittle fracture will happen. At lower temperatures, the BMGs with less free volume due to decrease of the mean atomic distances[1,2,16,17] will have less sites for STZ to initiate while larger activation energy will be needed. At a critical temperature, large shear stress is needed for the initiation of STZ, and the TTZ operation would be activated instead under tensile stress.

The DBT behavior of BMG related with the competition between the intrinsic shear strength τ_0 and cleavage strength σ_0 at different temperatures. Here, interestingly, for metallic glasses (amorphous alloys), it is the critical tensile strength σ_0 rather than critical shear strength τ_0 is closely related with temperature. For crystalline alloys, the shear stress for dislocation emission of bcc metals is markedly temperature dependent, in particular, at low temperatures, while the crack propagation stress (normal stress) is relatively independent of temperature. In the case of BMGs, the decrease of temperature will impede the mobility of the free-volume zones and result in the enhanced activation energy of a STZ, i.e., larger shear stress to initiate STZ then shear bands. While, the reason of high degree of atomic scale spatial fluctuations due to

decreasing temperature might be the origin of the decrease for the critical tensile strength σ_0 and is required to be further investigated.

In summary, a significant DBT behavior of BMGs was identified: macroscopic fracture mode from ductile shear fracture to brittle normal tensile fracture and microscopic fracture feature from micron-scaled vein patterns to nano-scaled dimples even periodic corrugations. The DBT behavior of BMGs was found to relate with the competition between intrinsic critical shear strength τ_0 and critical tensile strength σ_0, decreasing temperature will enhance the critical shear strength $\tau_0$and reduce the critical tensile strength σ_0. The results might provide useful information for understanding the unique properties of BMGs.

The financial support from the National Natural Science Foundation of China (NSFC) under Grant Nos. 51171138, 51171137 and 11002144 is gratefully acknowledged. The work was supported by Ph.D. Programs Foundation of Ministry of Education of China (20110201110002). The authors also wish to express their special thanks for the support from the National Basic Research Program of China (Grant No. 2010CB631003). We thank Professor Jianhong Chen at Lanzhou University of Technology for critical reading of the manuscript.

[1]H. Li, C. Fan, K. Tao, H. Choo, and P. K. Liaw, Adv. Mater. **18**, 752 (2006).
[2]H. Li, K. Tao, C. Fan, P. K. Liaw, and H. Choo, Appl. Phys. Lett. **89**, 041921 (2006).
[3]Y. J. Huang, J. Shen, J. F. Sun, and Z. F. Zhang, Mater. Sci. Eng., A **498**, 203 (2008).
[4]A. Kawashima, Y. Zeng, M. Fukuhara, H. Kurishita, N. Nishiyama, H. Miki, and A. Inoue, Mater. Sci. Eng., A **498**, 475 (2008).
[5]K. S. Yoon, M. Lee, E. Fleury, and J. C. Lee, Acta Mater. **58**, 5295 (2010).
[6]A. Kawashima, Y. Yokoyama, I. Seki, H. Kurishita, M. Fukuhara, H. Kimura, and A. Inoue, Mater. Trans. **50**, 2685 (2009).
[7]L. S. Huo, H. Y. Bai, X. K. Xi, D. W. Ding, D. Q. Zhao, W. H. Wang, R. J. Huang, and L. F. Li, J. Non-Cryst. Solids **357**, 3088 (2011).
[8]F. Jiang, M. Q. Jiang, H. F. Wang, Y. L. Zhao, L. He, and J. Sun, Acta Mater. **59**, 2057 (2011).
[9]R. Raghavan, P. Murali, and U. Ramamurty, Acta Mater. **57**, 3332 (2009).
[10]J. F. Knott, *Fundamentals of Fracture Mechanics* (Butterworth, London, 1973).
[11]P. Gumbsch, J. Riedle, A. Hartmaier, and H. F. Fischmeister, Science **282**, 1293 (1998).
[12]J. H. Chen, G. Li, R. Cao, and X. Y. Fang, Mater. Sci. Eng., A **527**, 5044 (2010).
[13]C. A. Schuh, A. C. Lund, and T. G. Nieh, Acta Mater. **52**, 5879 (2004).
[14]F. Spaepen, Acta Metall. **25**, 407 (1977).
[15]M. L. Falk, Phys. Rev. B **60**, 7062 (1999).
[16]B. P. Kanungo, M.S. thesis, Ohio State University, 2004.
[17]K. M. Flores, B. P. Kanungo, S. C. Glade, and P. Asoka-Kumar, J. Non-Cryst. Solids **353**, 1201 (2007).
[18]Z. F. Zhang, J. Eckert, and L. Schultz, Acta Mater. **51**, 1167 (2003).
[19]F. F. Wu, W. Zheng, S. D. Wu, Z. F. Zhang, and J. Shen, Int. J. Plast. **27**, 560 (2011).
[20]Z. F. Zhang, F. F. Wu, W. Gao, J. Tan, Z. G. Wang, M. Stoica, J. Das, J. Eckert, B. L. Shen, and A. Inoue, Appl. Phys. Lett. **89**, 251917 (2006).
[21]Z. F. Zhang, H. Zhang, B. L. Shen, A. Inoue, and J. Eckert, Philos. Mag. Lett. **86**, 643 (2006).
[22]Z. Bian, G. He, and G. L. Chen, Scr. Mater. **46**, 407 (2002).
[23]F. F. Wu, Z. F. Zhang, and S. X. Mao, Acta Mater. **57**, 257 (2009).
[24]M. Q. Jiang, Z. Ling, J. X. Meng, and L. H. Dai, Philos. Mag. **88**, 407 (2008).
[25]U. Ramamurty, M. L. Lee, J. Basu, and Y. Li, Scr. Mater. **47**, 107 (2002).
[26]X. K. Xi, D. Q. Zhao, M. X. Pan, W. H. Wang, Y. Wu, and J. J. Lewandowski, Phys. Rev. Lett. **94**, 125510 (2005).
[27]Z. F. Zhang, G. He, J. Eckert, and L. Schultz, Phys. Rev. Lett. **91**, 045505 (2003).
[28]A. Christiansen and J. B. Shortall, J. Mater. Sci. **11**, 1113 (1976).
[29]Z. F. Zhang and J. Eckert, Phys. Rev. Lett. **94**, 094301 (2005).